IL-10–producing B cells are enriched in murine pericardial adipose tissues and ameliorate the outcome of acute myocardial infarction

Lan Wu[a,1], Rajeev Dalal[a], Connie D. Cao[a], J. Luke Postoak[a], Guan Yang[a], Qinkun Zhang[b], Zhizhang Wang[c], Hind Lal[b], and Luc Van Kaer[a,1]

[a]Department of Pathology, Microbiology, and Immunology, Vanderbilt University Medical Center, Nashville, TN 37232; [b]Division of Cardiovascular Medicine, Department of Medicine, Vanderbilt University Medical Center, Nashville, TN 37232; and [c]Vanderbilt–NIH Mouse Metabolic Phenotyping Center, Vanderbilt University Medical Center, Nashville, TN 37232

Edited by Ajay Chawla, University of California, San Francisco, CA, and accepted by Editorial Board Member Philippa Marrack September 13, 2019 (received for review July 9, 2019)

Acute myocardial infarction (MI) provokes an inflammatory response in the heart that removes damaged tissues to facilitate tissue repair/regeneration. However, overactive and prolonged inflammation compromises healing, which may be counteracted by antiinflammatory mechanisms. A key regulatory factor in an inflammatory response is the antiinflammatory cytokine IL-10, which can be produced by a number of immune cells, including subsets of B lymphocytes. Here, we investigated IL-10–producing B cells in pericardial adipose tissues (PATs) and their role in the healing process following acute MI in mice. We found that IL-10–producing B cells were enriched in PATs compared to other adipose depots throughout the body, with the majority of them bearing a surface phenotype consistent with $CD5^+$ B-1a cells ($CD5^+$ B cells). These cells were detected early in life, maintained a steady presence during adulthood, and resided in fat-associated lymphoid clusters. The cytokine IL-33 and the chemokine CXCL13 were preferentially expressed in PATs and contributed to the enrichment of IL-10–producing $CD5^+$ B cells. Following acute MI, the pool of $CD5^+$ B cells was expanded in PATs. These cells accumulated in the infarcted heart during the resolution of MI-induced inflammation. B cell-specific deletion of IL-10 worsened cardiac function, exacerbated myocardial injury, and delayed resolution of inflammation following acute MI. These results revealed enrichment of IL-10–producing B cells in PATs and a significant contribution of these cells to the antiinflammatory processes that terminate MI-induced inflammation. Together, these findings have identified IL-10–producing B cells as therapeutic targets to improve the outcome of MI.

IL-10–producing B cells | $CD5^+$ B cells | inflammation | pericardial adipose tissues | acute myocardial infarction

Despite advances in prevention and treatment, acute myocardial infarction (MI) remains a leading cause of mortality and morbidity worldwide (1, 2), highlighting the need for new therapeutic strategies. Acute MI provokes a sterile inflammatory response that centers in the heart and involves primarily the innate branch and to a lesser degree the adaptive branch of the immune system (3–5). The early "inflammatory phase" is characterized by recruitment of proinflammatory cells and release of proinflammatory mediators. Although these events are critical for instigating tissue repair/regeneration by removing damaged tissues, overactive and prolonged proinflammatory reactions exacerbate myocardial injury and cardiac dysfunction, contributing to short- and long-term complications (6–8). As such, a balanced inflammatory phase and its timely termination move the healing process to the subsequent "proliferative phase," followed by a "maturation phase" when the tissue environment in the infarcted heart transitions to an antiinflammatory state to promote a repair/regeneration process. In this regard, immunotherapies targeting inflammation hold the potential of improving the outcome of acute MI. While recent studies have begun to investigate the underlying mechanisms (9–12), much remains to be learned regarding the cellular and molecular mechanisms that regulate the progression of MI-induced inflammation. In this context, studies have identified a beneficial role of the antiinflammatory cytokine IL-10 in the outcome of acute MI (13–17). However, the cellular sources and downstream targets of this cytokine, which collectively provide cardioprotection, remain to be delineated.

Mature B cells are classified into B-1 and B-2 cells based on a combination of surface phenotype and functional properties, and each class of B cells is comprised of distinct subsets (18–20). B-2 cells are often referred to as conventional B cells and make up the majority of the B cell pool in primary and secondary lymphoid organs. B-1 cells belong to a group of so-called "innate-like B cells" that respond well to innate signals, such as Toll-like receptor ligands and other conserved pathogen-derived molecular patterns. Earlier studies identified their preferential residence in coelomic cavities (21–24). Surface expression of CD5 further distinguishes B-1a ($CD5^+$) from B-1b ($CD5^-$) cells. In addition to their well-known function to produce antibodies, B cells fulfill a number of antibody-independent functions. Among the latter B cell properties is the release of cytokines that in turn regulate inflammation (25, 26). Subsets of B cells that release either pro- or antiinflammatory cytokines have been identified (25). Published studies have

Significance

Myocardial infarction (MI) remains a leading cause of mortality and morbidity worldwide. Although it is recognized that a balanced and timely terminated proinflammatory response following acute MI is essential in promoting tissue repair/regeneration, the underlying regulatory mechanisms are poorly defined. In this report, we show that IL-10–producing B cells in mice: 1) Are enriched in pericardial adipose tissues (PATs) and influenced by cytokines preferentially expressed in these tissues; 2) expand in PATs following MI and accumulate in the infarcted heart during the resolution of MI-induced inflammation; and 3) facilitate resolution of inflammation and reduce myocardial injury to preserve cardiac function after MI. These findings identify IL-10–producing B cells, in particular those in PATs, as therapeutic targets for MI.

Author contributions: L.W. and L.V.K. designed research; L.W., R.D., C.D.C., J.L.P., G.Y., Q.Z., and Z.W. performed research; L.W. and H.L. analyzed data; and L.W. and L.V.K. wrote the paper.

The authors declare no competing interest.

This article is a PNAS Direct Submission. A.C. is a guest editor invited by the Editorial Board.

[1]To whom correspondence may be addressed. Email: lan.wu.1@vumc.org or luc.van.kaer@vumc.org.

This article contains supporting information online at www.pnas.org/lookup/suppl/doi:10.1073/pnas.1911464116/-/DCSupplemental.

First published October 7, 2019.

implicated a pathogenic role in acute MI for B cell subsets producing proinflammatory cytokines (27, 28). While still under debate, the term "regulatory B cells" has been employed in recent years to describe B cell subsets that modulate inflammation through production of antiinflammatory cytokines, with IL-10–producing B cells as the best-studied subset (29–31). Based on their surface phenotype and response to stimuli that can resemble either B-1 or B-2 cells, it is likely that IL-10–producing B cells can differentiate along the developmental pathway for either the B-1 or the B-2 cell lineage (32, 33). Regardless of their lineage development, CD5-expressing B cells have a higher propensity for IL-10 production and this property has been associated with CD5 expression (34, 35). Indeed, studies have shown that $CD5^+$ B-1a cells are the main IL-10–producing B cells in the peritoneal cavity (PerC) (34). We and other investigators have recently reported that murine perigonadal visceral adipose tissues (VATs) in the abdominal cavity represent another site where B-1 cells preferentially reside. These adipose tissues contain a significant pool of IL-10–producing B cells that protect against obesity-induced inflammation, with the majority of them bearing a surface phenotype of $CD5^+$ B-1a cells (36, 37).

VATs are also present in the thoracic cavity. The adipose depots associated with the heart (CATs) include epicardial adipose tissues (EATs), located between the myocardium and visceral pericardium (epicardium) or around coronary arteries, and pericardial adipose tissues (PATs) located between the epicardium and parietal pericardium (38). The presence of significant quantities of both EATs and PATs in humans and large animals has been long recognized (39–41). In mice, EATs are scant but not absent, whereas PATs are readily discernible (41). It has been known that CATs house aggregates of leukocytes (42–44). More recently, these anatomical structures have been referred to as fat-associated lymphoid clusters (FALCs) (28, 45, 46) that belong to a group of physiological and inflammation-induced tertiary lymphoid tissues (47, 48). Detailed analyses of FALCs in murine mesenteric VATs reveal a predominance of B cells with a large proportion of B-1 cells that drastically expand in response to peritoneal inflammation (45). Along this line of research, studies have detected a high density of FALCs in murine PATs (45, 46). A recent report has also provided evidence for their expansion following acute MI (28).

Nevertheless, critical questions remain regarding B cells in CATs and their role in MI-induced inflammation. First, what is their prevalence and subset composition? Second, where do they reside? Third, how are they regulated? Finally, how do they respond to acute MI and contribute to the progression of the inflammatory response? In this study, we began to address these questions in mice focusing on PATs due to the scarcity of EATs. We report here that murine PATs contain a large pool of B cells, in particular B-1 cells, that reside in FALCs. This B cell compartment is enriched with IL-10–producing B cells, with the majority of them bearing a surface phenotype consistent with $CD5^+$ B-1a cells. $CD5^+$ B cells significantly expand in PATs following acute MI. They accumulate in the infarcted heart during the resolution of MI-induced inflammation. The presence of IL-10–producing B cells facilitates termination of the proinflammatory response and plays a beneficial role in myocardial injury and cardiac function.

Results

PATs Are Enriched with IL-10–Producing B Cells. We previously reported that the B cell compartment in murine perigonadal VATs was enriched with IL-10–producing B cells and the majority of them were $CD5^+$ B-1a cells (36). To assess whether this was reflected in adipose tissues throughout the body, we examined a variety of adipose depots. We harvested thoracic (pericardial and periaortic) (Fig. 1*A*) VATs, abdominal (perigonadal, retroperitoneal, and mesenteric) VATs, interscapular brown adipose tissues (BATs), and inguinal subcutaneous white adipose tissues (SATs) from adult WT C57BL/6J (WT B6) mice. We also included heart ventricles to pave the way for later studies evaluating acute MI. We purified stromal vascular fraction cells (SVFs) from the harvested tissues. For comparison, we collected PerC wash and conventional lymphoid organs (spleen and lymph nodes) and prepared single cells. We analyzed the B cell compartment by flow cytometry employing a commonly used strategy that was used in our previous studies (36) (Fig. 1*B*). We found that VATs in the thoracic cavity shared the characteristics of B cell subset composition with those in the abdominal cavity, in that they all contained a large proportion of B-1 cells that was split roughly 1:1 between B-1a and B-1b cells (*SI Appendix*, Table S1). The distribution of B cell subsets in VATs closely resembled the one in PerC but differed from the B cell subset distribution in other adipose depots, conventional lymphoid organs, and heart ventricles (*SI Appendix*, Table S1). The highest frequency of B cells in PATs among adipose depots drew our attention.

We further compared B cells in PATs with those in perigonadal VATs that we previously examined (36). While the distribution of B-1 and B-2 cells appeared similar in the 2 adipose depots, PATs had significantly higher prevalence of B-1a cells (Fig. 1*C*). In our pilot studies testing acute MI, we observed up-regulation of B220 on B cells in PATs of MI-operated mice (*SI Appendix*, Fig. S1*A*), which could be recapitulated on B cells in PerC after intraperitoneal injection of lipopolysaccharide (LPS) (*SI Appendix*, Fig. S1*B*). While the mechanism remains unclear, possibly due to the response by B cells to inflammation (49), it limited us in identifying B-1 cells and their subsets during acute MI utilizing the feature of the low to intermediate level of B220 expression on these cells (50). Because CD5 predominantly marks B-1a cells in the B cell compartment (50), we sought to examine $CD5^+$ B cells as a surrogate for B-1a cells (Fig. 1*B*). In PATs, the surface phenotype of $CD5^+$ B cells closely resembled the one on B-1a cells but differed from that on B-2 cells (*SI Appendix*, Fig. S2). Further delineating B-1 and B-2 cell subsets among $CD5^+$ B cells showed a predominance of the former subset (Fig. 1*D*). Having established this correlation, we quantified $CD5^+$ B cells. Consistent with our observations on B-1a cells (*SI Appendix*, Table S1), the prevalence of $CD5^+$ B cells was significantly higher in VATs than non-VATs and approached the one in PerC. In particular, PATs had the highest frequency of $CD5^+$ B cells among all adipose depots examined (Fig. 1*E*). Together with a significantly larger B cell compartment, these findings translated into a higher total number and a strikingly higher tissue density of $CD5^+$ B cells in PATs than in perigonadal VATs (Fig. 1*F*).

We next examined IL-10 production by subsets of B cells in PATs. We first employed a commonly used approach in studying IL-10–producing B cells that detects intracellular IL-10 (Fig. 2*A*). Consistent with the previous observations in perigonadal VATs and PerC (36, 51), we detected little IL-10 in freshly isolated B cells of WT B6 mice, either by evaluating mean fluorescence intensity of IL-10 labeling or quantifying cells stained for IL-10 ($IL\text{-}10^+$) (*SI Appendix*, Fig. S3). As this is an inherent feature of IL-10–producing B cells, we applied a commonly used short-term ex vivo manipulation to further ascertain IL-10 production using IL-10 knockout mice (IL-10 KO) as controls (36, 51). In doing this, we consistently detected a small fraction of $IL\text{-}10^+$ B cells after a 5-h culture when protein transport was suppressed by monensin, indicating a spontaneous low level of IL-10 production that reached the threshold for detection. The fraction of $IL\text{-}10^+$ B cells significantly increased upon challenge with a mixture of innate stimuli, PIL (phorbol myristate acetate, ionomycin, and LPS) (Fig. 2 *B*, *Left*). Subsets of B-2, B-1b, and B-1a cells all contributed to the pool of IL-10–producing B cells. Under unchallenged conditions, B-1a cells constituted the majority of IL-10–producing B cells. Challenge with PIL increased the contribution by B-2 and B-1b cells, but B-1a cells nevertheless remained the majority subset among IL-10–producing B cells (Fig. 2 *B*, *Right*). Considering the limitations in identifying B-1a cells during acute MI, we further examined the contributions by $CD5^+$ B cells to the pool of IL-10–producing B cells in PATs. Consistent with our observations based on surface phenotype (*SI Appendix*, Fig. S2), $CD5^+$ B cells faithfully represented B-1a cells (Fig. 2 *B*, *Right*). To confirm the above findings in another model, we analyzed IL-10 reporter mice (52). The results were consistent with those obtained in WT B6 mice (Fig. 2*C*). The higher frequency of $IL\text{-}10^+$ B cells in the absence of

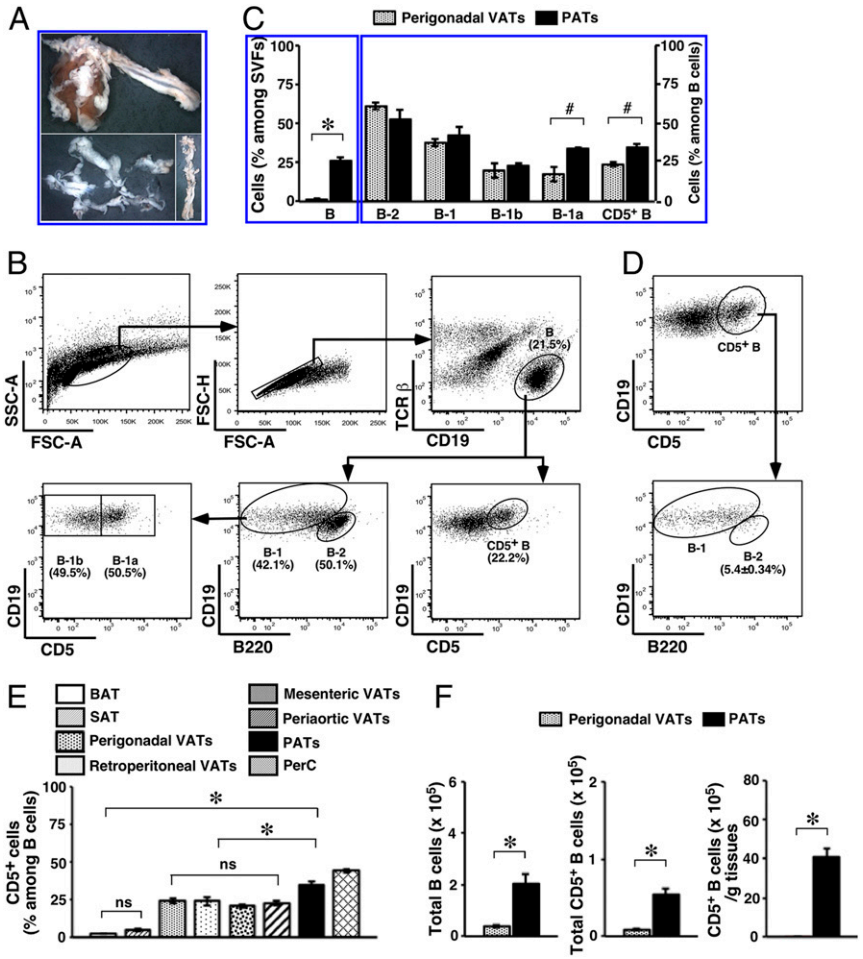

Fig. 1. B cell subsets in PATs. Adult WT B6 mice were used. (*A*) A heart and thoracic aorta with surrounding VATs are shown (*Upper*). PATs together with pericardium (*Lower Left*) or periaortic VATs (*Lower Right*) are shown (magnification: 0.5×). (*B*) Flow cytometry gating schemes for B cell subsets among SVFs are shown. (*C*) B cells (*Left*) and their subsets (*Right*) in the indicated adipose depots were examined (summary of 2 independent experiments, $n = 8$). (*D*) Representative flow cytometry plots are shown for the distribution of B-1 and B-2 cells among $CD5^+$ B cells in PATs. (*E*) The frequency of $CD5^+$ B cells in the indicated adipose depots and PerC were analyzed (summary of 2 independent experiments, $n = 8$). (*F*) Total B and $CD5^+$ B cells (*Left* and *Center*), and $CD5^+$ B cells per unit of tissues (*Right*) were compared between the indicated VAT depots (summary of 2 independent experiments, $n = 8$). $^{\#}P < 0.05$; $^{*}P < 0.01$; and ns, not statistically different; for all of the panels.

PIL (7.93 ± 1.37% in the IL-10 reporter group compared to 2.21 ± 0.32% in the WT B6 group, $P < 0.01$) might reflect the sensitivity of the former model in detecting IL-10.

We then analyzed IL-10 expression and secretion. For these purposes, we sorted B cells into different subsets using pooled PATs from WT B6 mice. To examine mRNAs by real-time PCR, we treated mice in vivo with LPS (53). The levels of IL-10 transcripts were not significantly different among subsets of B cells harvested from unstimulated mice, with the level in B-1a cells trending higher than in the other subsets. LPS treatment promoted significantly increased IL-10 gene transcription in B-1 cells and this was particularly the case for B-1a cells (Fig. 2*D*). To examine secreted IL-10, we cultured ex vivo the cells in the absence or presence of LPS and measured IL-10 released into the supernatant. The results are consistent with the observations in detecting intracellular IL-10, indicating a significantly higher competence of IL-10 production by B-1a cells than the other 2 subsets (Fig. 2*E*). The differences between IL-10 transcripts and secreted IL-10 observed under unstimulated conditions (Fig. 2 *D* and *E*, *Left*) might reflect a continuous release of IL-10 that accumulated in the culture supernatant. Together with the finding of a significantly larger B cell compartment compared to other adipose depots, our studies demonstrate that PATs are enriched with IL-10–producing B cells, with the majority of them being $CD5^+$ B cells. We performed additional experiments analyzing the B cell compartment in PATs, focusing on $CD5^+$ B cells.

$CD5^+$ B Cells Seed PATs Early in Life, Maintain a Steady Presence during Adulthood, and Reside in FALCs. To investigate the population dynamics of $CD5^+$ B cells in PATs, we examined WT B6 mice at different ages starting from weaning. In PATs, $CD5^+$ B cells were detected at the highest frequency when mice were 3 wk of age. This gradually decreased as mice matured to reach a steady state (Fig. 3*A*). Such age-related population dynamics appeared depot-specific but independent of their relationship with the body cavities. Seeding of $CD5^+$ B cells in perigonadal VATs lagged behind PATs. The frequency in the former depot increased as mice matured to reach a steady state (Fig. 3*A*). The frequency of $CD5^+$ B cells in thoracic periaortic VATs followed the pattern observed for perigonadal VATs, whereas the frequency of these cells in PerC resembled the one found in PATs (*SI Appendix*, Fig. S4). Total number of $CD5^+$ B cells expanded in both PATs and perigonadal VATs as the depots enlarged. However, only PATs maintained a higher tissue density of these cells (Fig. 3 *B* and *C*).

We then examined the tissue residence of B cells in PATs. We prepared whole-mount PATs and stained with H&E. As shown in *SI Appendix*, Fig. S5*A*, dense clusters of cells in different sizes and shapes were readily detectable. On H&E-stained sections, these clusters were embedded in or associated with adipose tissues (Fig. 3*D*). Oil red O staining of lipids confirmed the observations (*SI Appendix*, Fig. S5*B*). Similar to humans (54), murine PATs were comprised of adipocytes with either unilocular (white adipocytes) or multilocular (brown adipocytes) morphology (*SI Appendix*, Fig. S5*C*). The nonadipocyte clusters were always located in or associated with white adipose tissues (Fig. 3*D*). Immunocytochemistry showed that the vast majority of cells inside clusters expressed CD45, indicating a hematopoietic origin (*SI Appendix*, Fig. S5*D*). B cells were identified throughout the entire clusters (*SI Appendix*, Fig. S5*D*). Dual immunofluorescence staining confirmed the above findings (Fig. 3*E*). These results demonstrate that the densely packed cell clusters in PATs are indeed FALCs and contain abundant B cells. While our

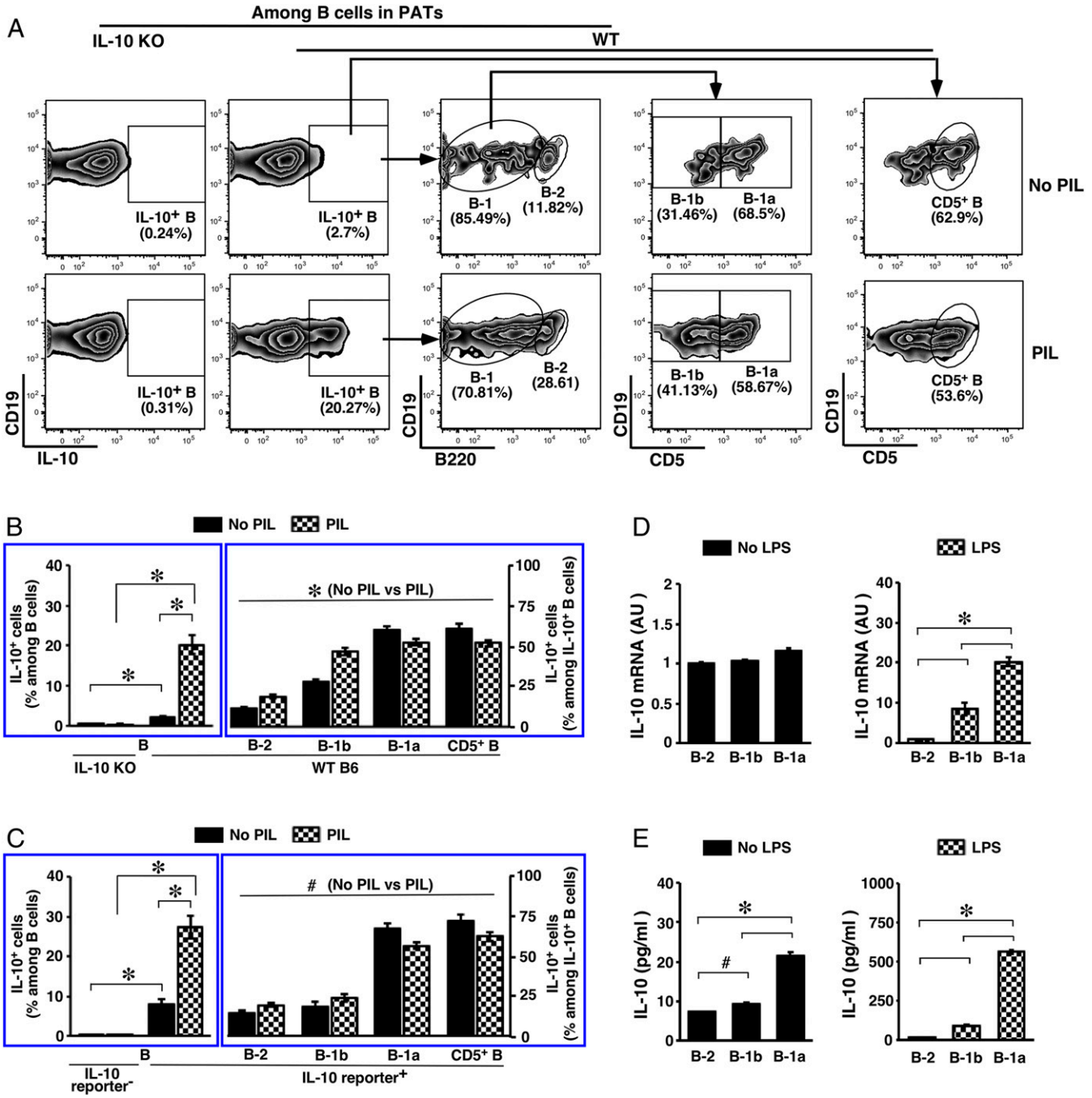

Fig. 2. IL-10–producing B cells in PATs. Adult WT B6 mice were used. (*A*) Flow cytometry gating schemes for subset distribution among IL-10–producing B cells in PATs are shown. (*B* and *C*) SVFs from PATs of mice with the indicated genotypes were cultured in the presence of the protein transport inhibitor monensin under the indicated stimulations. Cells were then examined for IL-10$^+$ B cells (*Left*) and subset distribution among IL-10$^+$ B cells (*Right*). Summary of 3 independent experiments is shown in *B* (n = 8 to 12), and summary of 2 independent experiments is shown in *C* (n = 6). (*D*) WT B6 mice were either left untreated (*Left*) or intraperitoneally injected with LPS (*Right*), and were killed 3 d later. SVFs from pooled PATs were sorted by flow cytometry to obtain subsets of B cells. Total RNAs from the sorted cells were used to detect IL-10 transcripts by real-time PCR. Results from 2 independent experiments are shown (AU, arbitrary unit). (*E*) SVFs from pooled PATs of WT B6 mice were sorted by flow cytometry to obtain subsets of B cells. Cells were cultured in the absence or presence of LPS for 48 h. IL-10 in the culture supernatant was then measured. $^{\#}P < 0.05$ and $^{*}P < 0.01$ for all of the panels.

earlier studies showed that the B cell pool in PATs is enriched with IL-10–producing B cells, formation of B cell-rich FALCs does not require IL-10, as evidenced by their presence in IL-10 KO mice (*SI Appendix*, Fig. S6). In addition to a large B cell compartment, PATs house a variety of other lymphoid cells as well as myeloid cells that are typically present in conventional lymphoid organs (*SI Appendix*, Fig. S7).

Although earlier investigations implicated self-renewal in postnatal maintenance of B-1a cells in PerC, later studies argued for a contribution by supplies from hematopoietic organs (55–58). We therefore performed experiments to gain insight into the postnatal maintenance of CD5$^+$ B cells in PATs, utilizing congenic B6 mice expressing either CD45.1 (CD45.1$^+$) or CD45.2 (CD45.2$^+$) to track cell origin. We first examined whether these cells were segregated

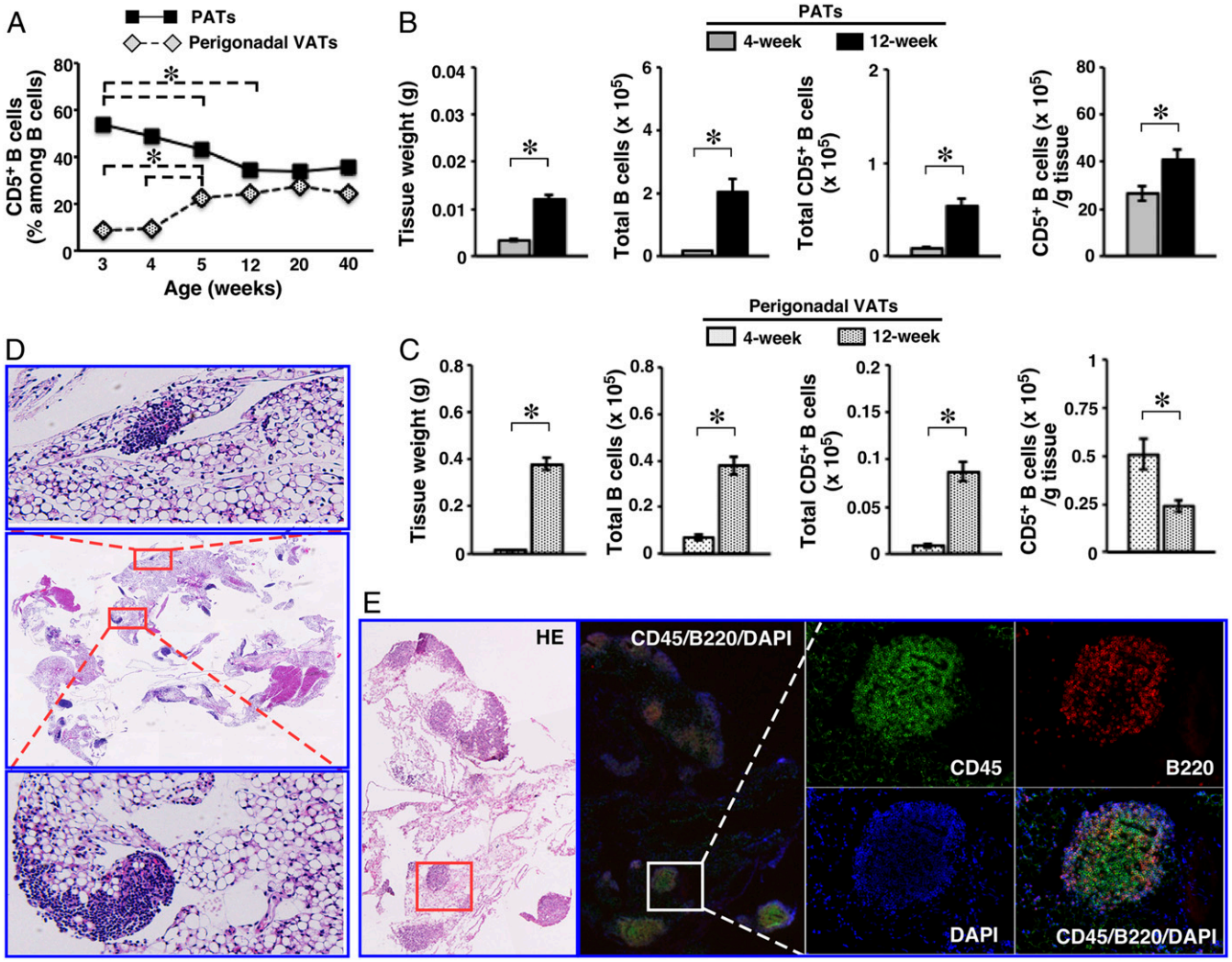

Fig. 3. Dynamics and residence of B cells in PATs. WT B6 mice were used. (*A*) Frequencies of $CD5^+$ B cells in the indicated adipose depots were examined at the indicated ages (summary of 2 independent experiments, $n = 8$ for each age). (*B* and *C*) The indicated parameters for B cells were examined in the indicated adipose depots of mice at 4 and 12 wk of age (summary of 2 to 3 independent experiments, $n = 11$ to 14). (*D*) Paraffin-embedded sections of PATs together with pericardium were stained with H&E (magnification: 0.5×). Two areas with densely packed cells are enlarged to show clusters. Representative graphs from 3 independent experiments are shown ($n = 6$). (*E*) Frozen sections of PATs together with pericardium were either stained with H&E or immunostained for the indicated markers (magnification: 4×). One area containing a FALC is enlarged to illustrate B cells. $^*P < 0.01$ for all of the panels.

between VATs in the 2 body cavities, namely PerC and the pleural cavity. We harvested B cells from PerC of $CD45.1^+$ donors and adoptively transferred equal numbers of B cells into the PerC, pleural cavity, or blood circulation of $CD45.2^+$ recipients. After 1 wk, we assayed the prevalence of donor-derived cells in PATs and perigonadal VATs (Fig. 4*A*). The results showed that subsets of B cells predominantly migrated to VATs within the cavity that received donor cells, making it unlikely that $CD5^+$ B cells in VATs enter the circulation and redistribute (Fig. 4 *B*, *Top* and *Middle*). This was confirmed by transferring B cells harvested from PATs into the PerC (*SI Appendix*, Fig. S8*A*).

Additionally, we obtained the following observations. First, B-1 cells had a higher homing capacity to VATs compared to B-2 cells and this was true for both B-1a and B-1b cells. Second, $CD5^+$ B cells faithfully represented B-1a cells in the donor–recipient setting (Fig. 4*B* and *SI Appendix*, Fig. S8*A*). Third, B cells from PerC distributed to both perigonadal VATs and PATs when they were placed in the circulation. However, a higher frequency of these cells appeared in the former depot (Fig. 4*B*), suggesting a homing preference to the body location in which they naturally reside. We were unable to assess this property for B cells harvested from PATs due to the limited number of cells retrievable.

We then examined whether an outside source contributed to the postnatal maintenance of $CD5^+$ B cells in PATs. For this purpose, we employed the parabiosis model and surgically joined a $CD45.1^+$ mouse with a $CD45.2^+$ mouse. After 1 mo of conjoined living, we analyzed the prevalence of $CD5^+$ B cells coming from the parabiotic partner. We obtained similar results in the 2 partner groups. We refer here to the $CD45.1^+$ mice as donors, and present below the results from the $CD45.2^+$ mice. Both T and B cells of the donor and recipient origins reached equilibrium in the blood. Distribution of donor-derived lymphocyte subsets appeared tissue-specific (*SI Appendix*, Fig. S8*B*). Compared to B-2 cells, a lower frequency of B-1 cells incorporated into the partner's blood and this was true for both B-1a and B-1b cells (Fig. 4*C*), consistent with a lower efficiency of B-1 cell progenitors in producing B-1 cells after birth (55, 56). The frequencies of B cell subsets were lower in tissues compared to blood, presumably reflecting their distribution among multiple tissues. Distribution of B cell subsets in PerC and PATs followed a pattern similar to that in blood, with a higher homing preference to PerC than to PATs (Fig. 4*C*). Again, the

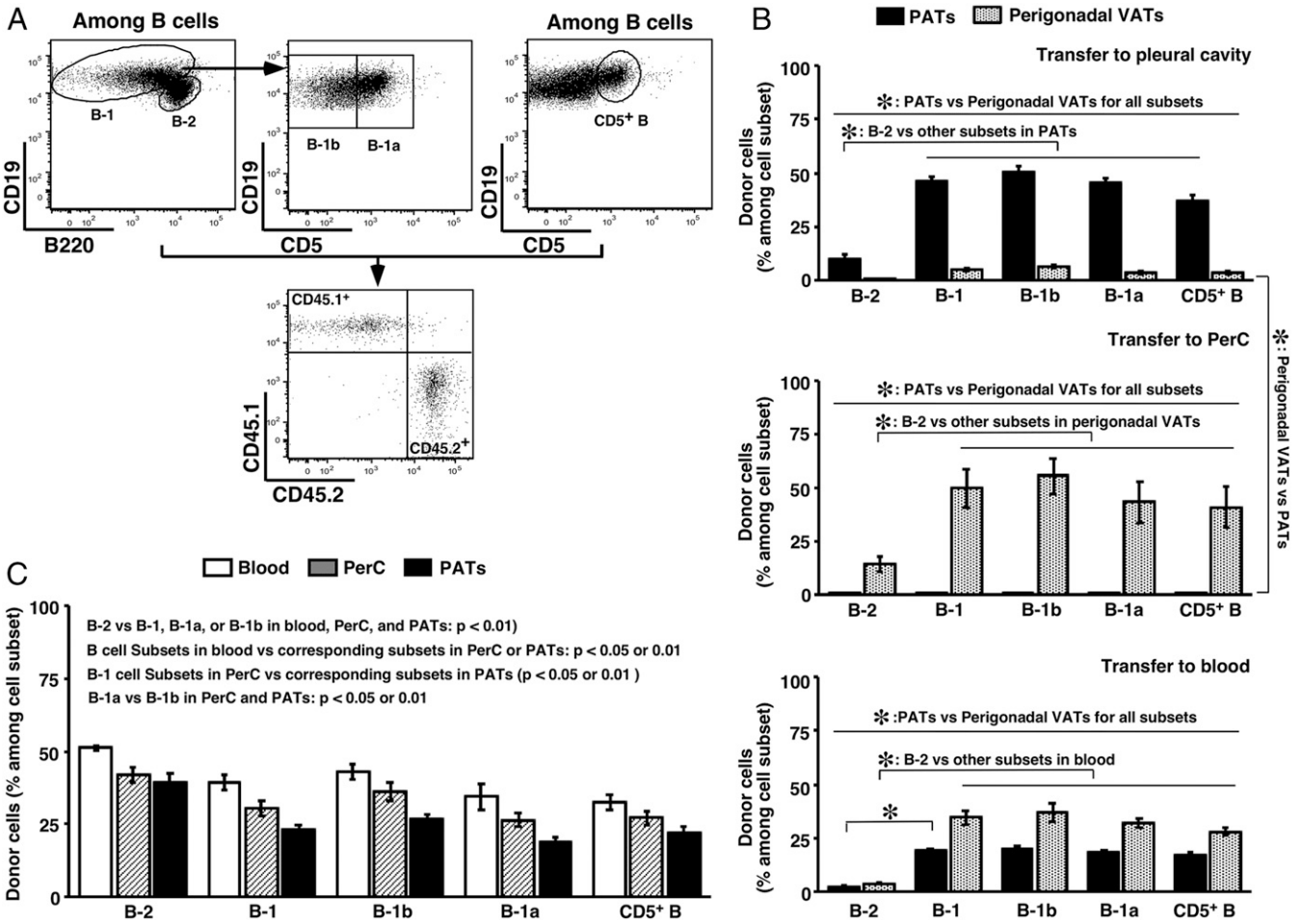

Fig. 4. Postnatal maintenance of the B cell compartment in PATs. Adult WT B6 mice were used. (*A*) Flow cytometry gating schemes for B cell subsets of donor/recipient origins are shown. (*B*) B cells from PerC of CD45.1$^+$ mice were injected into the indicated body locations of CD45.2$^+$ mice. Donor cells among subsets of B cells were examined in the indicated adipose depots (summary of 2 to 3 independent experiments, $n = 4$ to 8). (*C*) CD45.1$^+$ and CD45.2$^+$ mice were joined by parabiosis. CD45.1$^+$ cells among subsets of B cells in the indicated body locations of CD45.2$^+$ mice are shown (summary of 3 independent experiments, $n =$ 12 pairs). *$P < 0.01$ for all panels.

lower frequency of donor-derived B-1a compared to B-1b cells in the 2 body locations might reflect the lower potential of B-1a progenitors in producing mature cells after birth. Interestingly, B-1b cells appeared to have a higher homing capacity to both PerC and PATs than B-1a cells (Fig. 4*C*). Similar to the adoptive transfer model, CD5$^+$ B cells closely represented B-1a cells in the parabiosis model (Fig. 4*C*). The findings from our adoptive transfer experiments that CD5$^+$ B cells are retained in their home VATs, together with a sizable fraction of donor-derived CD5$^+$ B cells in PATs detected in the parabiosis experiments, argue for a contribution to the postnatal pool by a source outside of PATs. Taking these data together, we conclude that CD5$^+$ B cells seed FALCs of PATs early in life and maintain a steady presence throughout adulthood, and that the maintenance of a postnatal pool of these cells does not solely rely on self-renewal. We performed additional studies to gain insight into the mechanism that enriches these cells in PATs.

Preferential Expression of Cytokines Contributes to the Enrichment of IL-10–Producing CD5$^+$ B Cells in PATs. To explore the mechanism that enriches IL-10–producing B cells in PATs, we examined the cytokine IL-33 and the chemokine CXCL13 that play a critical role in B cell biology. IL-33 functions through ST2, a membrane-bound receptor (59). It promotes antibody production by B-1 cells in PerC and in FALCs of thoracic VATs (46, 60). CXCL13, on the other hand, acts via receptor CXCR5 (47, 48). It plays a critical role in the enrichment of B-1 cells in abdominal VATs (45, 61). Compared to perigonadal VATs, we found that both IL-33 and CXCL13 were highly expressed in PATs of WT B6 mice (Fig. 5*A*). This preferential expression appeared cytokine-specific. The levels of CXCL12 were similar between the 2 depots, whereas CCL2 trended lower in PATs (*SI Appendix*, Fig. S9*A*). To ascertain whether IL-33 regulates B cells in PATs, we analyzed IL-33 knockout mice (IL-33 KO) (62). Deficiency in this cytokine increased the prevalence of B cells, although this did not reach significance. Subset distribution in the B cell pool was altered, with significant decreases in B-1 cells affecting both B-1a and B-1b cells (Fig. 5*B*). Consequently, the prevalence of CD5$^+$ B cells was significantly reduced (Fig. 5*C*). Consistent with the differential expression pattern shown in Fig. 5*A*, absence of IL-33 did not affect the B cell compartment in perigonadal VATs at the age examined and this was reflected in the prevalence of CD5$^+$ B cells (Fig. 5*C*). Notably, IL-33 deficiency significantly reduced IL-10–producing B-1a cells, and hence IL-10–producing CD5$^+$ B cells, in PATs (Fig. 5*D*). Analyses of ST2 knockout mice (ST2 KO) (63) confirmed the role of IL-33 (*SI Appendix*, Fig. S9 *B* and *C*). ST2 expression levels on B cells were much lower than those detected on T cells in PATs under unstimulated conditions. However, consistent with previous findings on B-1 cells in PerC and spleen (60), in vivo stimulation with IL-33 enhanced ST2 expression on subsets of B-1 cells but not B-2 cells (*SI Appendix*, Fig. S10*A*). Interestingly, and again in line with prior studies in PerC and spleen (60), such treatment

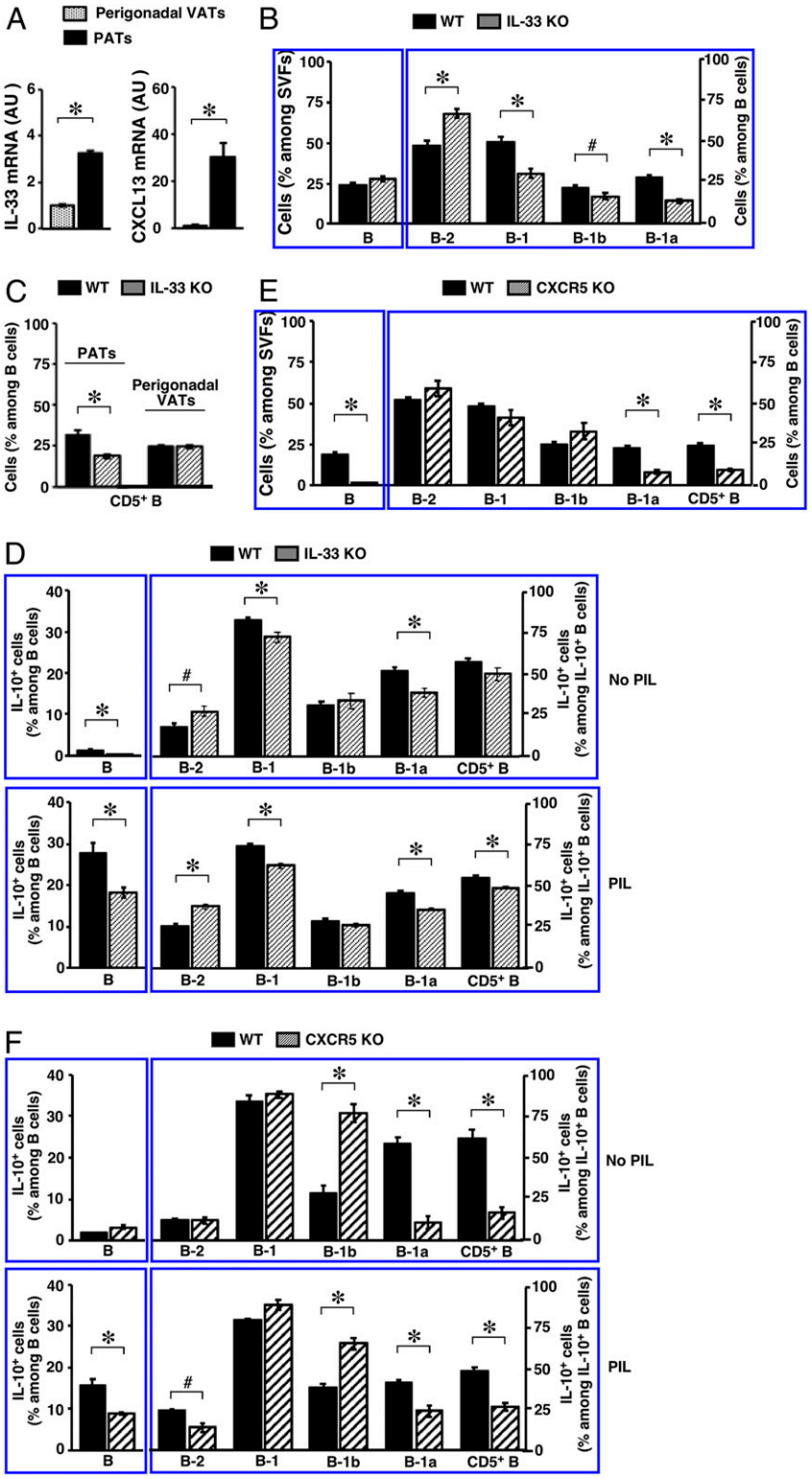

Fig. 5. Impact of cytokines on the B cell compartment in PATs. Adult mice were used. (*A*) Transcripts of the indicated genes in the indicated adipose depots of WT B6 mice were examined (summary of 2 independent experiments, $n = 8$; AU, arbitrary unit). (*B* and *E*) Frequencies of B cells (*Left*) and their subsets (*Right*) in PATs of mice with the indicated genotypes are shown (summary of 2 independent experiments, $n = 9$ to 12). (*C*) Frequencies of $CD5^+$ B cells in the indicated adipose depots of mice with indicated genotypes are shown (summary of 2 independent experiments, $n = 12$). (*D* and *F*) SVFs from PATs of mice with the indicated genotypes were treated as described in the legend for Fig. 2*B*, and examined for IL-10^+ B cells (*Left*) and subset distribution among IL-10^+ B cells (*Right*). Summaries of 2 independent experiments ($n = 9$ to 12) are shown. $^{\#}P < 0.05$ and $^{*}P < 0.01$ for all of the panels.

expanded B-1b cells (*SI Appendix*, Fig. S10*B*). Finally, we evaluated contributions by CXCL13. Because CXCL13 knockout mice are not readily available, we utilized CXCR5 knockout mice (CXCR5 KO), a strain deficient in the CXCL13 receptor and employed previously to examine B-1 cells in FALCs (45). Divergent from the observations with IL-33, absence of CXCL13 receptor signaling drastically decreased the prevalence of B cells in PATs. Among the remaining B cells, B-1a cells were significantly reduced and this was reflected in $CD5^+$ B cells (Fig. 5*E*). Accordingly, B-1a cells, and hence $CD5^+$ B cells, made significantly fewer contributions to the remaining IL-10–producing B cell pool in PATs of CXCR5 KO mice (Fig. 5 *F*, *Upper*). Upon ex vivo challenge with PIL, the overall IL-10 response by B cells was reduced in PATs of CXCR5 KO mice and this affected both B-2 and B-1a cells (Fig. 5 *F*, *Lower*). Altogether, these findings demonstrate that the preferentially

expressed IL-33 and CXCL13 enrich B-1a cells and promote their IL-10 production in PATs.

CD5$^+$ B Cells Expand in PATs following Acute MI and Accumulate in the Infarcted Heart during the Resolution of MI-Induced Inflammation. Compared to PATs, the normal mouse heart has a much lower prevalence of B cells. The frequency of B-1 cells, in particular B-1a cells, was significantly lower (*SI Appendix*, Table S1). CD5$^+$ B cells only represented a minor subset among B cells residing in the normal mouse heart (Fig. 6 *A*, *Bottom*). To investigate whether the B cell subsets in PATs play a role during acute MI, we employed a mouse model by surgically ligating the left anterior descending coronary artery (64). Similar to human pathology, such manipulation induces myocardial death in the left ventricle (LV) provoking an inflammatory response with dynamic alterations in subsets of immune cells (3–5). As such, we analyzed the B cell compartment in PATs and LVs following acute MI. Because of the challenge in identifying B-1 cells due to altered B220 expression in MI-operated mice, we quantified B cells and CD5$^+$ B cells. We performed sham or MI procedure on WT B6 mice, and killed them on days 3, 5, and 10 postsurgery to sample the progression from early inflammatory phase to subsequent proliferation and maturation phases (65). Acute MI dramatically expanded the size of SVFs in both PATs and LVs, which returned to baseline by day 10 (Fig. 6 *A*, *Top*). The frequencies of B cells were either unaltered or reduced, the latter presumably due to the expansion of myeloid cells such as monocytes (66). However, the size of B cell pools significantly enlarged by day 5 and returned to baseline by day 10 in both PATs and LVs (Fig. 6 *A*, *Middle*). Divergent from the dynamics of overall B cells, alterations in CD5$^+$ B cells displayed a differential pattern. Whereas they followed a similar dynamic in PATs as those observed for total B cells, the frequency and total number of CD5$^+$ B cells rose in infarcted LVs by day 5 and remained elevated at day 10 (Fig. 6 *A*, *Bottom*), indicating accumulation of these cells when the tissue environment shifted toward an antiinflammatory state. Histological analyses confirmed expansion of B cell-rich FALCs in PATs of MI-operated mice (Fig. 6*B*).

Consistent with the studies in PATs of normal mice, IL-10 was undetectable in B cells freshly purified from PATs and LVs of sham- or MI-operated mice regardless of the time point examined (*SI Appendix*, Fig. S11). The response of IL-10 production by B cells to ex vivo challenge with PIL displayed differential profiles for PATs and LVs during the proliferation phase. When they were examined at day 7 postsurgery, IL-10–producing B cells were reduced in PATs but increased in LVs, and the latter was accompanied by increases in IL-10–producing CD5$^+$ B cells (Fig. 6*C*). These results imply that IL-10–producing B cells, in particular those from the CD5$^+$ B cell fraction, expand in PATs and are recruited to the infarcted heart when the tissue environment transitions toward an antiinflammatory state. We employed 2 approaches to explore this scenario. First, we surgically removed PATs in mice undergoing MI and examined B cells in LVs 7 d later. We detected significant reductions in the frequency and total number of CD5$^+$ B cells, whereas the total B cell pool was not significantly altered (Fig. 6*D*), consistent with recruitment of the former subset from PATs to the infarcted heart. Because we have shown that CD5$^+$ B cells are well retained but can migrate to VATs within a particular body cavity, we next adoptively transferred CD45.1$^+$ B cells into the pleural cavity of CD45.2$^+$ mice undergoing sham or MI surgery. We then analyzed the B cell compartment in PATs and LVs 7 d postsurgery. Donor CD5$^+$ B cells (CD45.1$^+$) migrated to both PATs and LVs of sham-operated mice. In response to acute MI, significantly more donor CD5$^+$ B cells infiltrated LVs accompanied by a reduction of these cells in PATs (Fig. 6*E*). Together, the above findings support that acute MI expands IL-10–producing B cells, in particular those from the CD5$^+$ B cell fraction, in PATs and these cells are recruited to the infarcted heart.

B Cell-specific Deletion of IL-10 Worsens Cardiac Function after MI, Exacerbates Myocardial Injury, and Delays Resolution of Inflammation. We next investigated whether IL-10–producing B cells afford protection following acute MI. For this purpose, we employed a loss-of-function approach to delete IL-10 in B cells. A commonly used approach for examining IL-10–producing B cells consists of mixed bone marrow chimeras following lethal irradiation and marrow transplantation (67–70). Because we have shown that B cells, in particular B-1 cells, in PATs do not solely rely on self-renewal for postnatal maintenance, we reasoned that all subsets of B cells in PATs could repopulate from the transplanted marrow but that certain subsets might not fully reconstitute. To test this, we generated B6 mice containing IL-10–deficient B cells (B-IL-10 KO) and control mice containing IL-10–sufficient B cells (B-WT). We included age- and sex-matched untreated WT mice in this set of experiments. We examined the B cell compartment in PATs 8 wk after the transplantation procedure. All subsets of B cells reconstituted to a similar degree between the B-WT and B-IL-10 KO groups, indicating that deficiency of IL-10 in B cells did not interfere with the reconstitution process. The efficiency of B-1 cell reconstitution was significantly lower than for B-2 cells, and this primarily affected B-1a cells and was reflected in CD5$^+$ B cells (Fig. 7*A*). Whereas IL-10–producing B cells were indeed absent in B-IL-10 KO mice, they were able to repopulate PATs in B-WT mice. The prevalence of IL-10–producing B cells in B-WT mice did not reach the level found in WT mice and this was likely due to a lower prevalence of B-1a cells (Fig. 7*B*). As such, subsets of B cells were represented in the PATs of B-WT and B-IL-10 KO mice but the latter mice were deficient in IL-10–producing B cells. The reduced prevalence of B-1a cells might be due to their higher dependence on self-renewal of those that were generated during the fetal and neonatal period but were eliminated by lethal irradiation. Having established this, we then performed MI surgery on B-WT and B-IL-10 KO mice. We employed echocardiography to examine the function of LVs 3 wk post-MI (71). Lack of IL-10–producing B cells worsened the function of LVs after acute MI. This was reflected by a lower ejection fraction and a lower fractional shortening, which were calculated from the parameters taken from M-mode images (Fig. 7*C* and *SI Appendix*, Fig. S12). Masson's trichrome staining of collagen showed larger scars in the hearts of B-IL-10 KO mice, indicating exacerbated myocardial injury (Fig. 7*D*).

Acute MI provokes a sequential accumulation of 2 subsets of monocytes in the infarcted hearts (9, 66). Proinflammatory Ly-6C^{hi} monocytes dominate the early phase to promote removal of damaged tissues, whereas accumulation of antiinflammatory Ly-6C^{lo} monocytes during the later proliferation and maturation phases benefits repair. To begin investigations into a regulatory role of IL-10–producing B cells in MI-induced inflammation, we analyzed monocyte subsets in the infarcted LVs of B-WT and B-IL-10 KO mice. We employed the flow cytometry strategy (66) that was used in our previous studies on perigonadal VATs (36). This analysis separated monocytes from other lymphoid and myeloid cells and further specified the 2 subsets of monocytes (Fig. 7*E*). The results showed that influx of Ly-6C^{hi} monocytes was comparable between the 2 groups at day 3 post-MI, suggesting that lack of IL-10–producing B cells did not impair MI-induced proinflammatory monocyte response. However, the clearance of these cells was significantly delayed in B-IL-10 KO mice, as reflected by a higher prevalence of Ly-6C^{hi} monocytes at day 10 post-MI (Fig. 7 *E*, *Right*). Interestingly, the prevalence of Ly-6C^{lo} monocytes was significantly lower in B-IL-10 KO mice at day 3 post-MI, implicating a slower transition to an antiinflammatory tissue environment in the infarcted LVs (Fig. 7 *E*, *Right*). These results support a regulatory role of IL-10–producing B cells on the MI-induced monocyte response. Finally, the overall tissue environment remained more proinflammatory in the infarcted LVs of B-IL-10 KO mice 2 wk post-MI. The proinflammatory cytokines TNF-α and IL-18 remained significantly higher and IL-6 trended higher as well (Fig. 7*F*). The above findings demonstrate a beneficial role of IL-10–producing B cells in acute MI, facilitating the termination of MI-induced inflammation to protect against myocardial injury and to preserve cardiac function. They also implicate a regulatory role of these cells on other inflammatory cells involved in MI-induced inflammation.

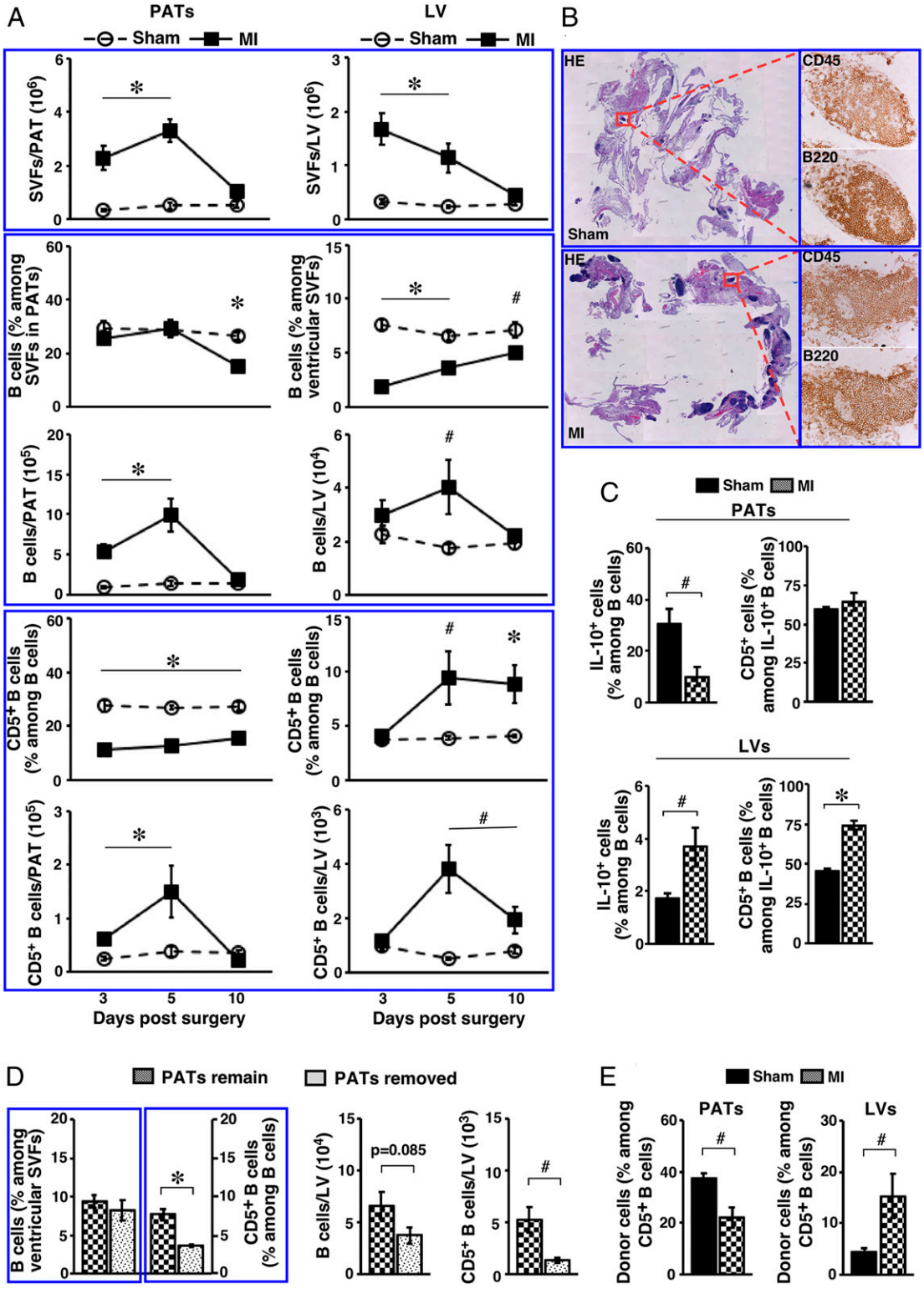

Fig. 6. Impact of acute MI on the B cell compartment in PATs and LVs. Adult WT B6 mice were used. (*A*) SVFs from the indicated tissues of mice that underwent the indicated treatment were examined at the indicated time postsurgery. Summary of 2 to 3 independent experiments ($n = 8$ to 12 at each time point) for the indicated parameters are shown. (*B*) Sham- or MI-operated mice were examined 5 d postsurgery. Serial paraffin-embedded sections of PATs together with pericardium were either stained with H&E (*Left*, magnification: 0.5×) or immunostained for the indicated markers (*Right*, magnification: 20×). Representative graphs from 2 independent experiments are shown ($n = 4$). (*C*) Mice underwent the indicated surgery and were analyzed 7 d postsurgery. SVFs from the indicated tissues were cultured as described in the legend for Fig. 2*B*, in the presence of PIL. Cells were examined for IL-10$^+$ B cells (summary of 2 independent experiments, $n = 6$). (*D*) Mice underwent the indicated procedures in conjunction with acute MI, and were examined 7 d later. Frequencies (*Left*) and total numbers (*Right*) of B cells and CD5$^+$ B cells in LVs are shown (summary of 2 independent experiments, $n = 6$). (*E*) B cells from PerC of CD45.1$^+$ mice were transferred into the pleural cavity of CD45.2$^+$ mice during sham or MI surgery. Mice were examined 7 d later for donor cells among CD5$^+$ B cells in the indicated tissues (summary of 3 independent experiments, $n = 7$). $^{\#}P < 0.05$ and $^{*}P < 0.01$ for all panels.

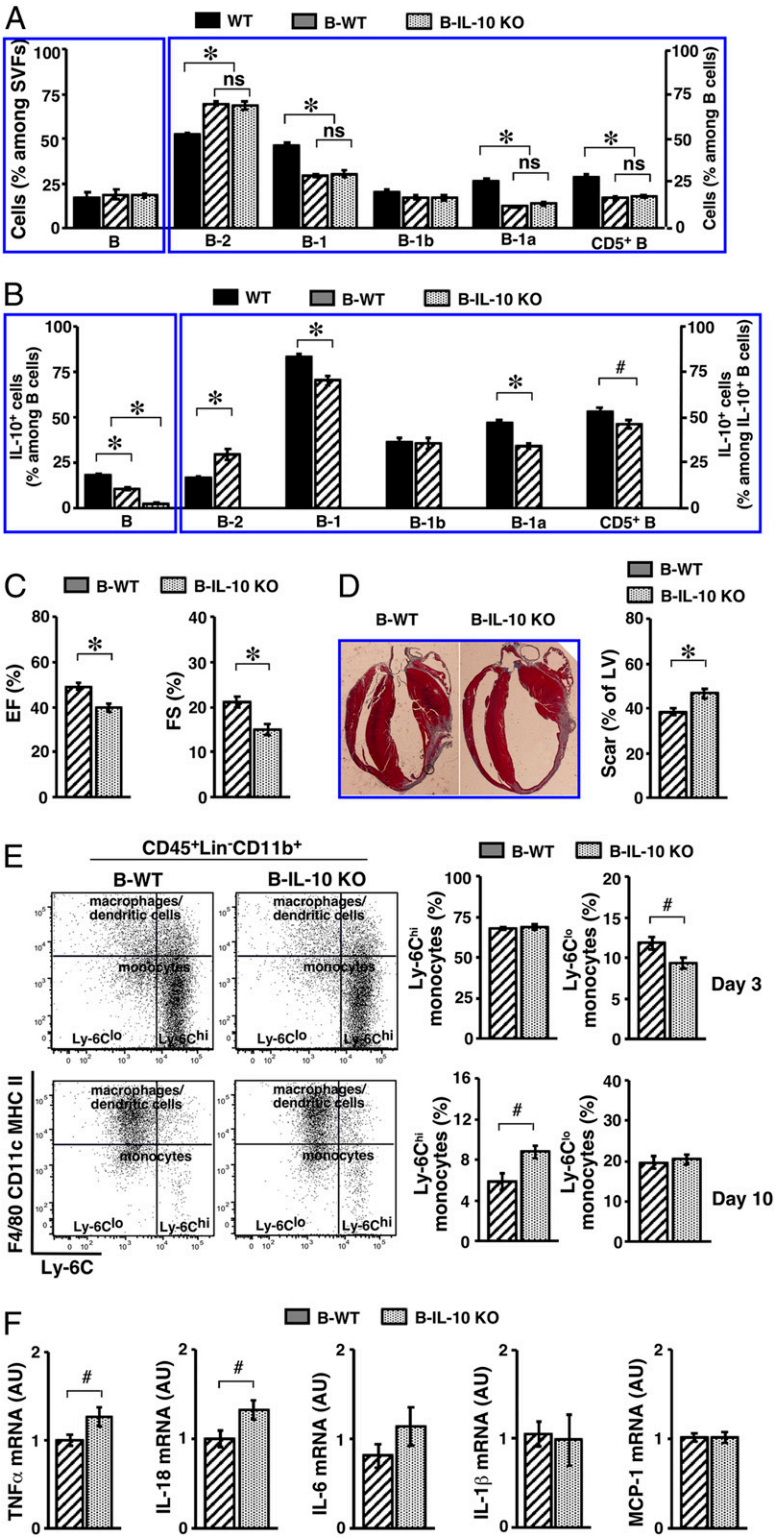

Fig. 7. Impact of B cell IL-10 deficiency on the outcome of acute MI. (*A*) WT B6 mice were either left untreated (WT), or underwent bone marrow transplantation to generate B-WT or B-IL-10 KO mice. SVFs from PATs were analyzed for frequencies of B cells (*Left*) and their subsets (*Right*). Summary of 2 independent experiments ($n = 5$ to 7) is shown. (*B*) Mice were treated as described in *A*. SVFs from PATs were cultured as described in the legend for Fig. 2*B*, in the presence of PIL. Cells were examined for IL-10$^+$ B cells (*Left*) and subset distribution among IL-10$^+$ B cells (*Right*). A summary of 2 independent experiments is shown ($n = 5$ to 7). (*C*) B-WT and B-IL-10 KO mice underwent MI surgery, and were examined for LV function by echocardiography 3 wk later. Ejection fraction (EF, *Left*) and fractional shortening (FS, *Right*) are shown ($n = 13$ to 17). (*D*) Mice were treated as described in *C*, and were killed 3 wk later. Representative images of Masson's trichrome stain are shown (*Left*) (magnification: 0.5×). Scar areas were measured and are presented as percent of LV circumference (*Right*) (summary of 3 independent experiments, $n = 17$). (*E*) Mice underwent MI and were killed at the indicated time points postsurgery. SVFs from LVs were analyzed for subsets of monocytes. Representative flow cytometry plots at the indicated time points are shown (*Left*). Frequencies of monocyte subsets at the indicated time points are shown (*Right*) (summary of 2 independent experiments, $n = 8$ for each time point). (*F*) Transcripts of the indicated genes in LVs of mice were examined by real-time PCR 2 wk post-MI. Summary of 2 independent experiments is shown ($n = 7$ to 11). $^{\#}P < 0.05$ and $^{*}P < 0.01$ for all panels.

Discussion

We report here that murine PATs are enriched with IL-10–producing B cells that reside in FALCs. The majority of them at this tissue location are CD5$^+$ B cells. The preferentially expressed cytokines IL-33 and CXCL13 contribute to the enrichment of IL-10–producing CD5$^+$ B cells in PATs. In response to acute MI, these cells significantly expand in PATs. They are recruited to the infarcted heart during the resolution of MI-induced inflammation. The presence of IL-10–producing B cells improves the outcome of acute MI, by facilitating termination of MI-induced inflammation to minimize myocardial injury and preserve cardiac function. The role of IL-10 in acute MI has drawn research attention in recent years. Despite some inconsistencies in the published findings (72), a large body of evidence supports a beneficial role of this cytokine (13–17). Our studies now specify subsets of B cells as one of the cellular

sources for IL-10, which are enriched in the adipose tissues wrapped around the heart.

Our study shows that $CD5^+$ B cells populate PATs early in life and are maintained at a steady presence throughout adulthood. Based on their surface phenotype and their response to MI-induced sterile inflammation, these cells likely differentiate along the developmental pathway for the B-1a cell lineage (19, 33). In adult mice, these cells appear to be segregated among different body cavities but can migrate to the VATs within the respective body cavity. In addition to a self-renewal property described by earlier studies for B-1a cells, our studies show that the postnatal maintenance of $CD5^+$ B cells in PATs does not solely rely on self-renewal. Our finding that $CD5^+$ B cells are enriched in PATs and reside in FALCs is reminiscent of prior studies on B-1 cells in FALCs of mesenterium (45). This is not particularly surprising, considering the shared developmental origin of these tissues from the splanchnopleuric mesoderm. Interestingly, it has been shown that this intraembryonic region contains progenitors for B-1a cells (73). PATs may have evolved in the thoracic cavity as part of the surveillance mechanism for inflammatory insults, similar to the mesenterium and omentum in the abdominal cavity (74). Additional investigation is needed to address whether IL-10–producing $CD5^+$ B cells in PATs contain a distinct fraction of B-1a cells that can further expand upon pathological challenge. Alternatively, it remains possible that all B-1a cells in PATs are capable of proliferating and producing IL-10 upon exposure to particular signals. Similarly, it remains possible that subsets of B-2 cells, such as $CD5^+$ B10 cells, contribute to the pool of IL-10–producing $CD5^+$ B cells in PATs. Our findings on a lower frequency of $CD5^+$ B-1a cells that are incorporated into PATs of the parabiotic partners are in line with a lower potential of B-1a progenitors in producing mature cells after birth. Alternatively, these observations may simply reflect a different kinetics of lifespan and turnover for B-1a cells. Additional studies are needed to ascertain these scenarios.

It has been reported that subsets of B cells that produce proinflammatory cytokines worsen the outcome of acute MI by promoting the early inflammatory phase and the recruitment of proinflammatory myeloid cells following MI (27, 28). Opposing effects of proinflammatory and IL-10–producing B cells have been observed for several chronic inflammatory diseases, such as obesity (36, 75). Our studies now extend this concept to the pathophysiology of acute MI. Our findings indicate that IL-10–producing B cells facilitate termination of MI-induced inflammation and impact the balance between pro- and antiinflammatory monocytes after acute MI. In addition to our findings, previous studies have implicated IL-10 in other downstream cellular targets of hematopoietic and nonhematopoietic origins (15, 16). A better understanding of the interactions between IL-10–producing B cells and other cell types relevant to the progression of MI-induced inflammation posting the potential of identifying new targets for prevention and treatment of acute MI. Considering the opposing roles for the different subsets of B cells in MI-induced inflammation, therapeutic strategies that promote IL-10–producing B cells or suppress proinflammatory B cells may be worthwhile to explore.

Our studies indicate that IL-33 is preferentially expressed in PATs. Signaling by this cytokine enriches B-1 cells at this adipose depot, influencing both B-1a and B-1b cells. It promotes IL-10–producing B-1a cells upon pathological challenge. Additional research is needed to examine the underlying mechanisms. It is likely that a variety of cell types in PATs express IL-33, as this was previously documented for IL-33 produced in abdominal VATs (59). The immediate cellular targets of IL-33 in PATs are also unclear. Innate lymphoid type 2 cells (ILC2s) are the best-studied IL-33–responding cells. In response to IL-33, these cells release type 2 cytokines, such as IL-5, to influence downstream target cells (59). In addition to ILC2s, several other cell types can respond to IL-33 to release type 2 cytokines (59). This includes B-1 cells, in particular B-1b cells (60). As such, it remains possible that B-1b cells and ILC2s in PATs respond to IL-33 to release type 2 cytokines. The latter might then act on $CD5^+$ B cells, in a manner similar to the response of B-1a cells in PerC (76, 77). Our studies also reveal a role for CXCL13, which is highly expressed in PATs. Divergent from IL-33, signaling by this chemokine enriches overall B cells in PATs. In addition to the impact on B-1a cells, CXCL13 also influences the contribution by B-2 cells to the IL-10–producing B cell pool. Considering the established regulatory role of these cytokines on B cells in conventional lymphoid organs, understanding the mechanism of action for each cytokine and the cooperation among these cytokines presents opportunities for unveiling new therapeutic targets.

The reported findings place IL-10–producing B cells in the antiinflammatory network that terminates MI-induced inflammation to facilitate tissue repair/regeneration. They identify a preferential residence of these cells in the adipose tissues surrounding the heart. Together, these results point to IL-10-producing B cells in PATs as therapeutic targets to improve the outcome of acute MI.

Materials and Methods

Mice. The following mouse strains of both sexes were used for this study. C57BL/6J (stock #000664, WT B6, $CD45.2^+$), B6 CD45.1 (stock #002014, $CD45.1^+$), IL-10 KO (stock #002251), μMT KO (stock #002288), IL-10 reporter (stock #008379), and CXCR5 KO (stock #006659) mice on the B6 background were from The Jackson Laboratory. IL-33 KO and ST2 KO mice on the B6 background were obtained from Michael Rosen, Cincinnati Children's Hospital Medical Center, Cincinnati, OH, with permission from Susumu Nakae, RIKEN Center for Life Science Technologies, Hyogo, Japan, and Dr. Andrew McKenzie, Medical Research Council Laboratory of Molecular Biology, Cambridge, United Kingdom, respectively. Mice were fed with a regular chow diet (5LOD, Labdiet) and water ad libitum, maintained on a 12-h light/dark cycle under specific pathogen-free conditions, and examined at 10 to 15 wk of age or at the ages specified for individual experiments. Age- and sex-matched mice between the experimental and control groups were used in each experiment.

Study Approval. All procedures for use of mice in the study were approved by the Institutional Animal Care and Use Committee at Vanderbilt University School of Medicine.

Reagents and Experimental Procedures. Details of reagents and experimental procedures are provided in *SI Appendix*.

ACKNOWLEDGMENTS. We thank Drs. Michael Rosen, Susumu Nakae, and Andrew McKenzie for providing IL-33 KO and ST2 KO mice on the B6 background. This work was supported by NIH Grants R01DK081536 (to L.W. and L.V.K.), R01DK104817 and R01AI139046 (to L.V.K.), R01HL133290 and R01HL119234 (to H.L.); and American Heart Association Grant 19TPA34910078 (to L.V.K.). R.D. and C.D.C. were medical students from New York Institute of Technology College of Osteopathic Medicine and Rutgers Robert Wood Johnson Medical School, respectively, who participated in the NIH/National Institute of Diabetes and Digestive and Kidney Diseases-sponsored Vanderbilt Medical Student Research Training Program (T35DK07383). J.L.P. was supported by institutional training Grants T32HL069765 and T32AR059039. FACS sorting was performed in the Flow Cytometry Shared Resource at Vanderbilt University Medical Center, supported by the Vanderbilt Ingram Cancer Center (P30 CA68485) and the Vanderbilt Digestive Disease Research Center (DK058404). Imaging was performed in the Cell Imaging Shared Resource at Vanderbilt University Medical Center, supported by the Vanderbilt Diabetes Research and Training Center (DK020593) and the Vanderbilt Ingram Cancer Center (P30 CA68485). Pericardial adipose tissues removal followed by acute myocardial infarction was performed by the Cardiovascular Physiology Core at Vanderbilt University Medical Center.

1. E. J. Benjamin *et al.*; American Heart Association Statistics Committee and Stroke Statistics Subcommittee, Heart disease and stroke statistics-2017 update: A report from the American Heart Association. *Circulation* **135**, e146–e603 (2017).
2. G. A. Roth *et al.*, Global and regional patterns in cardiovascular mortality from 1990 to 2013. *Circulation* **132**, 1667–1678 (2015).
3. N. G. Frangogiannis, The inflammatory response in myocardial injury, repair, and remodelling. *Nat. Rev. Cardiol.* **11**, 255–265 (2014).
4. F. K. Swirski, Inflammation and repair in the ischaemic myocardium. *Hamostaseologie* **35**, 34–36 (2015).
5. U. Hofmann, S. Frantz, Role of T-cells in myocardial infarction. *Eur. Heart J.* **37**, 873–879 (2016).

6. M. G. Sutton, N. Sharpe, Left ventricular remodeling after myocardial infarction: Pathophysiology and therapy. *Circulation* **101**, 2981–2988 (2000).
7. A. M. van der Laan, M. Nahrendorf, J. J. Piek, Healing and adverse remodelling after acute myocardial infarction: Role of the cellular immune response. *Heart* **98**, 1384–1390 (2012).
8. P. S. Jhund, J. J. McMurray, Heart failure after acute myocardial infarction: A lost battle in the war on heart failure? *Circulation* **118**, 2019–2021 (2008).
9. M. Nahrendorf *et al*., The healing myocardium sequentially mobilizes two monocyte subsets with divergent and complementary functions. *J. Exp. Med.* **204**, 3037–3047 (2007).
10. J. Weirather *et al*., Foxp3+ CD4+ T cells improve healing after myocardial infarction by modulating monocyte/macrophage differentiation. *Circ. Res.* **115**, 55–67 (2014).
11. M. A. Sobirin *et al*., Activation of natural killer T cells ameliorates postinfarct cardiac remodeling and failure in mice. *Circ. Res.* **111**, 1037–1047 (2012).
12. M. Shiraishi *et al*., Alternatively activated macrophages determine repair of the infarcted adult murine heart. *J. Clin. Invest.* **126**, 2151–2166 (2016).
13. J. S. Burchfield *et al*., Interleukin-10 from transplanted bone marrow mononuclear cells contributes to cardiac protection after myocardial infarction. *Circ. Res.* **103**, 203–211 (2008).
14. Z. Yang, B. Zingarelli, C. Szabó, Crucial role of endogenous interleukin-10 production in myocardial ischemia/reperfusion injury. *Circulation* **101**, 1019–1026 (2000).
15. M. Jung *et al*., IL-10 improves cardiac remodeling after myocardial infarction by stimulating M2 macrophage polarization and fibroblast activation. *Basic Res. Cardiol.* **112**, 33 (2017).
16. P. Krishnamurthy *et al*., Interleukin-10 deficiency impairs bone marrow-derived endothelial progenitor cell survival and function in ischemic myocardium. *Circ. Res.* **109**, 1280–1289 (2011).
17. P. Krishnamurthy *et al*., IL-10 inhibits inflammation and attenuates left ventricular remodeling after myocardial infarction via activation of STAT3 and suppression of HuR. *Circ. Res.* **104**, e9–e18 (2009).
18. A. Kantor, A new nomenclature for B cells. *Immunol. Today* **12**, 388 (1991).
19. D. Allman, S. Pillai, Peripheral B cell subsets. *Curr. Opin. Immunol.* **20**, 149–157 (2008).
20. R. Berland, H. H. Wortis, Origins and functions of B-1 cells with notes on the role of CD5. *Annu. Rev. Immunol.* **20**, 253–300 (2002).
21. N. Baumgarth, The double life of a B-1 cell: Self-reactivity selects for protective effector functions. *Nat. Rev. Immunol.* **11**, 34–46 (2011).
22. J. F. Kearney, Innate-like B cells. *Springer Semin. Immunopathol.* **26**, 377–383 (2005).
23. D. Parra *et al*., Pivotal advance: Peritoneal cavity B-1 B cells have phagocytic and microbicidal capacities and present phagocytosed antigen to CD4+ T cells. *J. Leukoc. Biol.* **91**, 525–536 (2012).
24. A. Meyer-Bahlburg, D. J. Rawlings, Differential impact of Toll-like receptor signaling on distinct B cell subpopulations. *Front. Biosci.* **17**, 1499–1516 (2012).
25. P. Shen, S. Fillatreau, Antibody-independent functions of B cells: A focus on cytokines. *Nat. Rev. Immunol.* **15**, 441–451 (2015).
26. X. Zhang, Regulatory functions of innate-like B cells. *Cell. Mol. Immunol.* **10**, 113–121 (2013).
27. Y. Zouggari *et al*., B lymphocytes trigger monocyte mobilization and impair heart function after acute myocardial infarction. *Nat. Med.* **19**, 1273–1280 (2013).
28. M. Horckmans *et al*., Pericardial adipose tissue regulates granulopoiesis, fibrosis, and cardiac function after myocardial infarction. *Circulation* **137**, 948–960 (2018).
29. E. C. Rosser, C. Mauri, Regulatory B cells: Origin, phenotype, and function. *Immunity* **42**, 607–612 (2015).
30. Z. Vadasz, T. Haj, A. Kessel, E. Toubi, B-regulatory cells in autoimmunity and immune mediated inflammation. *FEBS Lett.* **587**, 2074–2078 (2013).
31. K. M. Candando, J. M. Lykken, T. F. Tedder, B10 cell regulation of health and disease. *Immunol. Rev.* **259**, 259–272 (2014).
32. A. B. Kantor, L. A. Herzenberg, Origin of murine B cell lineages. *Annu. Rev. Immunol.* **11**, 501–538 (1993).
33. R. R. Hardy, K. Hayakawa, B cell development pathways. *Annu. Rev. Immunol.* **19**, 595–621 (2001).
34. A. O'Garra *et al*., Ly-1 B (B-1) cells are the main source of B cell-derived interleukin 10. *Eur. J. Immunol.* **22**, 711–717 (1992).
35. H. Gary-Gouy *et al*., Human CD5 promotes B-cell survival through stimulation of autocrine IL-10 production. *Blood* **100**, 4537–4543 (2002).
36. L. Wu, V. V. Parekh, J. Hsiao, D. Kitamura, L. Van Kaer, Spleen supports a pool of innate-like B cells in white adipose tissue that protects against obesity-associated insulin resistance. *Proc. Natl. Acad. Sci. U.S.A.* **111**, E4638–E4647 (2014).
37. L. Shen *et al*., B-1a lymphocytes attenuate insulin resistance. *Diabetes* **64**, 593–603 (2015).
38. G. Iacobellis, Epicardial and pericardial fat: Close, but very different. *Obesity (Silver Spring)* **17**, 625, author reply 626–627 (2009).
39. J. M. Marchington, C. A. Mattacks, C. M. Pond, Adipose tissue in the mammalian heart and pericardium: Structure, foetal development and biochemical properties. *Comp. Biochem. Physiol. B* **94**, 225–232 (1989).
40. D. Corradi *et al*., The ventricular epicardial fat is related to the myocardial mass in normal, ischemic and hypertrophic hearts. *Cardiovasc. Pathol.* **13**, 313–316 (2004).
41. Y. Yamaguchi *et al*., Adipogenesis and epicardial adipose tissue: A novel fate of the epicardium induced by mesenchymal transformation and PPARγ activation. *Proc. Natl. Acad. Sci. U.S.A.* **112**, 2070–2075 (2015).
42. T. Nakatani, H. Shinohara, Y. Fukuo, S. Morisawa, T. Matsuda, Pericardium of rodents: Pores connect the pericardial and pleural cavities. *Anat. Rec.* **220**, 132–137 (1988).
43. Y. Fukuo, T. Nakatani, H. Shinohara, T. Matsuda, The mouse pericardium: It allows passage of particulate matter from the pleural to the pericardial cavity. *Anat. Rec.* **222**, 1–5 (1988).
44. K. Takada, Y. Otsuki, S. Magari, Lymphatics and pre-lymphatics of the rabbit pericardium and epicardium with special emphasis on particulate absorption and milky spot-like structures. *Lymphology* **24**, 116–124 (1991).
45. C. Bénézech *et al*., Inflammation-induced formation of fat-associated lymphoid clusters. *Nat. Immunol.* **16**, 819–828 (2015).
46. L. H. Jackson-Jones *et al*., Fat-associated lymphoid clusters control local IgM secretion during pleural infection and lung inflammation. *Nat. Commun.* **7**, 12651 (2016).
47. M. J. Kain, B. M. Owens, Stromal cell regulation of homeostatic and inflammatory lymphoid organogenesis. *Immunology* **140**, 12–21 (2013).
48. C. D. Buckley, F. Barone, S. Nayar, C. Bénézech, J. Caamaño, Stromal cells in chronic inflammation and tertiary lymphoid organ formation. *Annu. Rev. Immunol.* **33**, 715–745 (2015).
49. I. Ubillos *et al*., Chronic exposure to malaria is associated with inhibitory and activation markers on atypical memory B cells and marginal zone-like B cells. *Front. Immunol.* **8**, 966 (2017).
50. F. L. Smith, N. Baumgarth, B-1 cell responses to infections. *Curr. Opin. Immunol.* **57**, 23–31 (2019).
51. T. Matsushita, T. F. Tedder, Identifying regulatory B cells (B10 cells) that produce IL-10 in mice. *Methods Mol. Biol.* **677**, 99–111 (2011).
52. M. Kamanaka *et al*., Expression of interleukin-10 in intestinal lymphocytes detected by an interleukin-10 reporter knockin tiger mouse. *Immunity* **25**, 941–952 (2006).
53. D. Maseda *et al*., Regulatory B10 cells differentiate into antibody-secreting cells after transient IL-10 production in vivo. *J. Immunol.* **188**, 1036–1048 (2012).
54. H. S. Sacks *et al*., Uncoupling protein-1 and related messenger ribonucleic acids in human epicardial and other adipose tissues: Epicardial fat functioning as brown fat. *J. Clin. Endocrinol. Metab.* **94**, 3611–3615 (2009).
55. B. L. Esplin, R. S. Welner, Q. Zhang, L. A. Borghesi, P. W. Kincade, A differentiation pathway for B1 cells in adult bone marrow. *Proc. Natl. Acad. Sci. U.S.A.* **106**, 5773–5778 (2009).
56. C. L. Barber, E. Montecino-Rodriguez, K. Dorshkind, Reduced production of B-1-specified common lymphoid progenitors results in diminished potential of adult marrow to generate B-1 cells. *Proc. Natl. Acad. Sci. U.S.A.* **108**, 13700–13704 (2011).
57. E. E. Ghosn, P. Sadate-Ngatchou, Y. Yang, L. A. Herzenberg, L. A. Herzenberg, Distinct progenitors for B-1 and B-2 cells are present in adult mouse spleen. *Proc. Natl. Acad. Sci. U.S.A.* **108**, 2879–2884 (2011).
58. S. Düber *et al*., Induction of B-cell development in adult mice reveals the ability of bone marrow to produce B-1a cells. *Blood* **114**, 4960–4967 (2009).
59. A. B. Molofsky, A. K. Savage, R. M. Locksley, Interleukin-33 in tissue homeostasis, injury, and inflammation. *Immunity* **42**, 1005–1019 (2015).
60. M. Komai-Koma *et al*., IL-33 activates B1 cells and exacerbates contact sensitivity. *J. Immunol.* **186**, 2584–2591 (2011).
61. J. Rangel-Moreno *et al*., Omental milky spots develop in the absence of lymphoid tissue-inducer cells and support B and T cell responses to peritoneal antigens. *Immunity* **30**, 731–743 (2009).
62. K. Oboki *et al*., IL-33 is a crucial amplifier of innate rather than acquired immunity. *Proc. Natl. Acad. Sci. U.S.A.* **107**, 18581–18586 (2010).
63. M. J. Townsend, P. G. Fallon, D. J. Matthews, H. E. Jolin, A. N. McKenzie, T1/ST2-deficient mice demonstrate the importance of T1/ST2 in developing primary T helper cell type 2 responses. *J. Exp. Med.* **191**, 1069–1076 (2000).
64. E. Gao *et al*., A novel and efficient model of coronary artery ligation and myocardial infarction in the mouse. *Circ. Res.* **107**, 1445–1453 (2010).
65. S. D. Prabhu, N. G. Frangogiannis, The biological basis for cardiac repair after myocardial infarction: From inflammation to fibrosis. *Circ. Res.* **119**, 91–112 (2016).
66. F. K. Swirski *et al*., Identification of splenic reservoir monocytes and their deployment to inflammatory sites. *Science* **325**, 612–616 (2009).
67. S. Fillatreau, C. H. Sweenie, M. J. McGeachy, D. Gray, S. M. Anderton, B cells regulate autoimmunity by provision of IL-10. *Nat. Immunol.* **3**, 944–950 (2002).
68. N. A. Carter *et al*., Mice lacking endogenous IL-10-producing regulatory B cells develop exacerbated disease and present with an increased frequency of Th1/Th17 but a decrease in regulatory T cells. *J. Immunol.* **186**, 5569–5579 (2011).
69. A. Ray, S. Basu, C. B. Williams, N. H. Salzman, B. N. Dittel, A novel IL-10-independent regulatory role for B cells in suppressing autoimmunity by maintenance of regulatory T cells via GITR ligand. *J. Immunol.* **188**, 3188–3198 (2012).
70. I. Hilgendorf *et al*., Innate response activator B cells aggravate atherosclerosis by stimulating T helper-1 adaptive immunity. *Circulation* **129**, 1677–1687 (2014).
71. S. Gao, D. Ho, D. E. Vatner, S. F. Vatner, Echocardiography in mice. *Curr. Protoc. Mouse Biol.* **1**, 71–83 (2011).
72. P. Zymek *et al*., Interleukin-10 is not a critical regulator of infarct healing and left ventricular remodeling. *Cardiovasc. Res.* **74**, 313–322 (2007).
73. I. E. Godin, J. A. Garcia-Porrero, A. Coutinho, F. Dieterlen-Lièvre, M. A. Marcos, Para-aortic splanchnopleura from early mouse embryos contains B1a cell progenitors. *Nature* **364**, 67–70 (1993).
74. S. Meza-Perez, T. D. Randall, Immunological functions of the omentum. *Trends Immunol.* **38**, 526–536 (2017).
75. D. A. Winer *et al*., B cells promote insulin resistance through modulation of T cells and production of pathogenic IgG antibodies. *Nat. Med.* **17**, 610–617 (2011).
76. K. Takatsu, S. Takaki, Y. Hitoshi, Interleukin-5 and its receptor system: Implications in the immune system and inflammation. *Adv. Immunol.* **57**, 145–190 (1994).
77. B. G. Moon, S. Takaki, K. Miyake, K. Takatsu, The role of IL-5 for mature B-1 cells in homeostatic proliferation, cell survival, and Ig production. *J. Immunol.* **172**, 6020–6029 (2004).